Photosensitized one-electron oxidation of DNA*

Kiyohiko Kawai and Tetsuro Majima‡

The Institute of Scientific and Industrial Research (SANKEN), Osaka University, Mihogaoka 8-1, Ibaraki, Osaka 567-0047, Japan

Abstract: Photosensitized one-electron oxidation of DNA has attracted much interest because it causes oxidative damage which leads to mutation, and because it is involved in the basic mechanism of photodynamic therapy. In the present article, we describe the mechanistic study of photosensitized DNA damage, especially addressing the kinetics of hole transfer by adenine(A)-hopping and its effect on the DNA damage. The combination of the transient absorption measurement and DNA damage quantification by high-performance liquid chromatography clearly demonstrate that the yield of the DNA damage correlates well with the lifetime of the charge-separated state caused by A-hopping, showing that hole transfer helps DNA damage. These findings led us to propose a new method to accomplish the efficient DNA damage using a combination of two-color, two-laser irradiation.

Keywords: DNA; DNA damage; one-electron oxidation; photosensitized oxidation; hole transfer in DNA; charge-separated state; two-color, two-laser irradiation; photosensitized electron transfer.

INTRODUCTION

The one-electron oxidation of DNA occurs during photoirradiation in the presence of photosensitizers (Sens) and has been extensively studied because it leads to the formation of oxidative lesions that cause carcinogenesis and aging [1,2]. Photosensitized DNA damage has also received attention from a therapeutic point of view, since DNA is one of the potential targets of photodynamic therapy [3]. The electron-rich nucleobases are prime targets for photosensitized one-electron oxidation. Among the four DNA bases, guanine (G) exhibits the lowest oxidation potential as shown in Fig. 1 [4,5]. Therefore, G
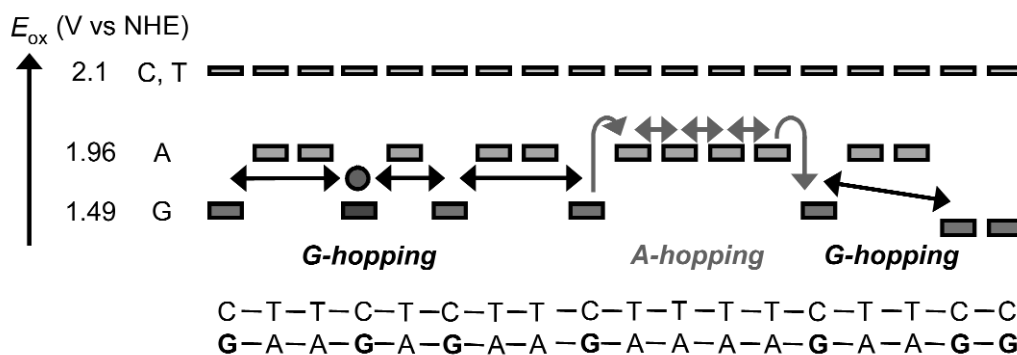
Fig. 1 Oxidation potentials of nucleobases and schematic representation of hole transfer in DNA by G-hopping and A-hopping.

is the most subjective to the one-electron oxidation, forming the radical cation of guanine ($G^{\bullet+}$), of which reaction with water and molecular oxygen leads to the formation of mutagenic oxidative products.

At the end of the 1990s, it was demonstrated that $G^{\bullet+}$ or a hole migrate through DNA over a long distance (~200 Å) by hopping between Gs [6–9], and the kinetics and biological consequences of hole transfer in DNA have become a topic of interest and research. From the spectroscopic measurements of the hole transfer in DNA, Lewis et al. determined the rate constants of the hole transfer between Gs across one A–T base pair to be in the range of 10^6–10^8 s^{-1} [10]. The rate constant for the single-step charge-transfer process (k_{ct}) usually follows an exponential dependence on the donor–acceptor distance Δr (eq. 1). The distance dependence parameter β in eq. 1

$$\ln k_{ct} \propto -\beta \Delta r \tag{1}$$

has been determined as 0.6 $Å^{-1}$ in DNA [11–13]. Judging from these rates and the β-value of 0.6 $Å^{-1}$, hole transfer between Gs separated by more than four A–T base pairs should be too slow to compete with the hole-trapping reactions. However, strand cleavage experiments revealed the occurrence of the long-range hole transfer in DNA containing long intervening A–T sequences between Gs [7,8]. Giese et al. pointed out the role of adenine (A), the second most easily oxidized base, and explained this contradiction by showing that hole transfer can be mediated by thermally induced hopping between As (A-hopping) [14]. Thus, the hole transfer in DNA has been demonstrated to occur by the two different mechanisms, G-hopping (superexchange between Gs across the intervening A–T bridge) and A-hopping [charge is carried by the bridge base A as its radical cation ($A^{\bullet+}$)] as shown in Fig. 1. Considering the low efficient endothermic oxidation of A by $G^{\bullet+}$ and the weak distance dependence of A-hopping, it was suggested that once after the generation of $A^{\bullet+}$ the hopping between A proceeds fast [15]. Such a fast hole transfer may promote photosensitized DNA damage by separating the hole and $Sens^{\bullet-}$ during the photosensitized one-electron oxidation of DNA, providing the time for $G^{\bullet+}$ and $Sens^{\bullet-}$ to react with water or O_2. However, little was known about the kinetics of A-hopping, and its effect on the photosensitized DNA damage. Herein, we describe the kinetics of A-hopping in DNA based on the transient absorption measurements, and the significance of A-hopping on the photosensitized DNA damage. We also demonstrate the new methodology to increase the efficiency of photosensitized DNA damage, which utilizes the combination of two-color, two-laser irradiation.

KINETICS OF HOLE TRANSFER IN DNA BY ADENINE HOPPING

In this section, we present the transient absorption measurements of hole transfer in DNA. Hairpin oligodeoxynucleotides (ODNs) possessing naphthaldiimide (NDI) at the hairpin loop as a photosensitizer for hole injection and phenothiazine (PTZ) at the 5'-end as a hole acceptor were synthesized [16,17]. Since the reduction potential of NDI in the singlet excited state ($^1NDI^*$) is 2.7 V (vs. SCE in DMSO), $^1NDI^*$ can oxidize A (E_{ox} = 1.7 V vs. SCE in DMSO) to trigger A-hopping [4,5,17] and be eventually trapped at PTZ [18].

The sequence of the synthetic hairpin ODN and chemical structures of NDI and PTZ are shown in Table 1 and Fig. 2, respectively. HPAn (n = 4–8) was designed to investigate the intrastrand A-hopping, and HPATn and HPGn were made to examine the interstrand A-hopping and the influence of a G as a hole trap in the A_n sequences, respectively. NDI has been reported to serve as a linker to form a stable hairpin DNA [17]. The circular dichroism (CD) spectra for the entire NDI- and PTZ-modified hairpin ODNs studied here showed maxima around 280 and minima around 250 nm which are characteristic of B-DNA. They had melting temperatures higher than 45 °C, which was independent of the DNA concentration. These results clearly indicate the formation of a stable hairpin structure.

Table 1 Quantum yield of charge separation (Φ_{cs}), and rate constant of charge recombination (k_{cr}) in NDI- and PTZ-modified hairpin ODNs.

ODN	Sequence	$\Phi_{cs}{}^{a}/10^{-2}$	$k_{cr}{}^{b}/10^{5}$ s^{-1}
HPA4	[5']PTZ–AAAA–NDI–TTTT[3']	2.1	7.5
HPA5	[5']PTZ–AAAAA–NDI–TTTTT[3']	1.4	1.7
HPA6	[5']PTZ–AAAAAA–NDI–TTTTTT[3']	1.0	0.40
HPA7	[5']PTZ–AAAAAAA–NDI–TTTTTTT[3']	0.85	0.12
HPA8	[5']PTZ–AAAAAAAA–NDI–TTTTTTTT[3']	0.65	0.03
HPAT1	[5']PTZ–ATATA–NDI–TATAT[3']	0.39	2.1
HPAT2	[5']PTZ–ATATATA–NDI–TATATAT[3']	0.13	0.40
HPG1	[5']PTZ–AGAGA–NDI–TCTCT[3']	0.37	0.64
HPG2	[5']PTZ–AAGAA–NDI–TTCTT[3']	0.75	0.66

[a]Determined from the transient absorption of the triplet benzophenone as an actinometer during the 355-nm laser flash photolysis.
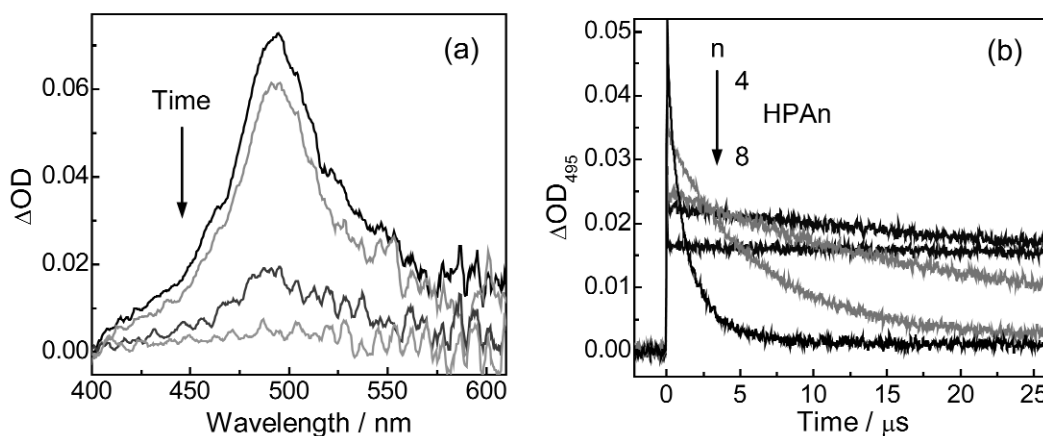[b]Obtained from the decay of the transient absorption of NDI$^{\bullet-}$ at 495 nm.
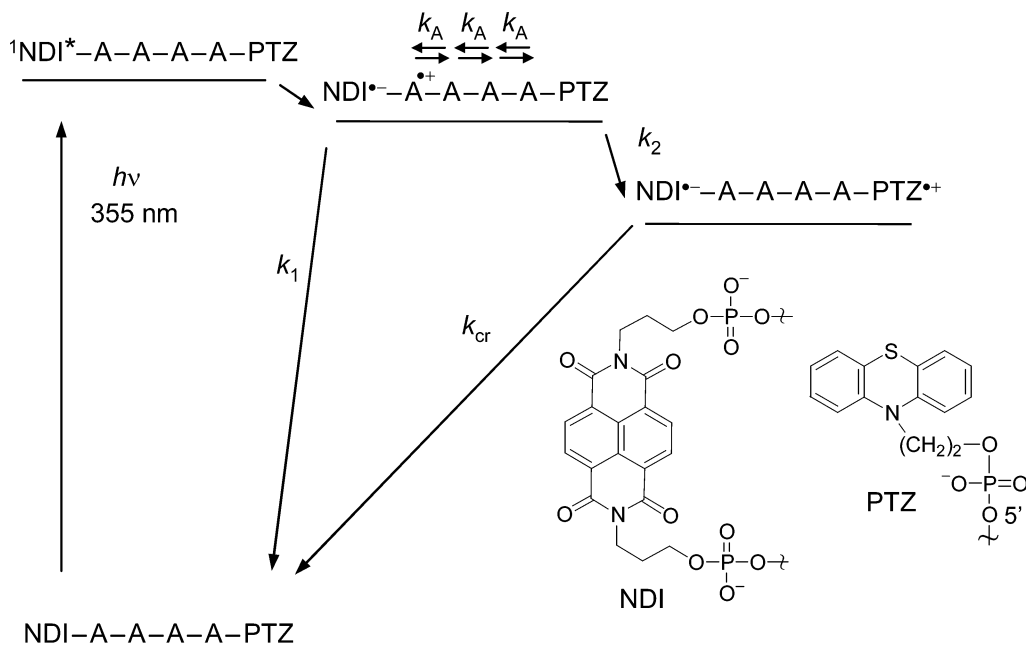
Fig. 2 Chemical structures of NDI, PTZ, and kinetic scheme for the charge separation and charge recombination in NDI- and PTZ-modified hairpin ODN.

Kinetic scheme for the charge separation and recombination processes after the 355-nm laser flash of hairpin ODN modified with the NDI and PTZ are shown in Fig 2. Almost no fluorescence was observed for these hairpin ODNs, suggesting the rapid electron-transfer quenching of ^{1}NDI* in accord with the previous report [17]. Since the NDI is adjacent to the A–T base pair, and the oxidation potential of A (E_{ox} = 1.7 V vs. SCE in DMSO) is lower than that of T [4], it is probable that the electron transfer from ^{1}NDI* to the nearest A occurs immediately after the excitation, resulting in the formation of NDI radical anion (NDI$^{\bullet-}$) and A$^{\bullet+}$. Accordingly, the charge separation between NDI and PTZ is con-

sidered to occur via the A-hopping process between As as shown in Fig. 2. On the other hand, the charge recombination between $NDI^{•-}$ and $PTZ^{•+}$ is expected to occur via the single-step superexchange mechanism because $PTZ^{•+}$ cannot oxidize A.

The charge separation and recombination processes between NDI and PTZ after the 355-nm laser excitation (full width at half-height of 8 ns, 5 mJ/pulse) were examined by monitoring the formation and decay of the $NDI^{•-}$, respectively. In the case of HPA5, a transient absorption spectrum with a peak at 495 nm was observed immediately after the flash excitation (Fig. 3a). This transient absorption spectrum was assigned to $NDI^{•-}$ of $NDI^{•-}-A_5-PTZ^{•+}$ [19], demonstrating the charge separation process via the A-hopping. In contrast, no transient absorption spectrum was observed for the hairpin ODN possessing only NDI, suggesting that the PTZ worked as a hole trap to inhibit the charge recombination process between $NDI^{•-}$ and $A^{•+}$, and that A-hopping occurs very fast within the pulse duration of 5 ns. Unfortunately, we could not distinguish the transient absorption of $PTZ^{•+}$ from that of $NDI^{•-}$ because the molar extinction coefficient of the $PTZ^{•+}$ (1×10^4 M^{-1} cm^{-1} at 520 nm) [20] is much smaller than that of $NDI^{•-}$ (1×10^5 M^{-1} cm^{-1} at 495 nm) [19]. Thus, $NDI^{•-}$ in the charge-separated state was mainly observed in the transient absorption measurement.

Fig. 3 (a) Transient absorption spectra of HPA5 obtained at 100 ns, 1, 10, and 100 µs after the 355-nm laser flash excitation in Ar-saturated solution containing 80 µM DNA, 20 mM Na phosphate buffer (pH 7.0), and 100 mM NaCl. (b) Decay profiles of the transient absorption measured at 495 nm for HPA*n* (*n* = 4–8).

The formation and decay of $NDI^{•-}$ for HPA*n* (*n* = 4–8) are shown in Fig. 3b. The quantum yields of the charge separation (Φ_{cs}) and rate constants for the charge recombination (k_{cr}) were determined by analyzing the formation of the transient absorption of $NDI^{•-}$ observed upon a laser flash (ΔOD_{495}) and the subsequent decay of $NDI^{•-}$, respectively (Table 1). These quantum yields decreased only slightly with the increasing number of A bases, while the decay rates strongly decreased as the number of A bases increased. The charge recombination rate slowed down and occurred in the time region of µs with the increasing number of A bases. Interestingly, the charge-separated state persisted over 300 µs when NDI and PTZ were separated by eight A bases. On the other hand, the charge separation yields dramatically decreased by changing the consecutive A sequence to the AT repeat sequence (HPAT1 and –AT2) or GC containing sequence (HPG1 and –G2). These results would be explained by the slower A-hopping for interstrand process and hole trapping by G, respectively. The interstrand A-hopping is likely to be much slower compared with the intrastrand process because of an absence of the direct stacking between As. A similar trend for the interstrand charge transfer was previously observed [21–23]. In the case of sequences containing Gs, G serves as a hole trap on the charge shift process because the oxidation potential of G is lower than A [5,24], causing inhibition of the A-hopping in which a hole migrates to PTZ. Higher charge separation yields for HPG2 than that for HPG1 would be attrib-

uted to the different location of G. This difference shows that a hole is trapped at G more distant from the NDI in the case of HPG2 compared to that of HPG1, causing a slower charge recombination between NDI$^{\bullet-}$ and G$^{\bullet+}$. Hence, the consecutive A sequence is important for the effective A-hopping.

To elucidate the mechanism of the charge separation and recombination processes between NDI and PTZ, the distance dependences of these processes were investigated. The charge recombination between NDI$^{\bullet-}$ and PTZ$^{\bullet+}$ was considered to occur via the superexchange mechanism. In this mechanism, the distance dependence on the charge recombination rate (k_{cr}) is expressed by eq. 2,

$$\ln k_{cr} \propto - \beta \Delta r \qquad (2)$$

where β is the distance dependence parameter and Δr is the distance between NDI and PTZ. A linear correlation between $\ln k_{cr}$ and Δr was obtained to provide the β-value of 0.4 Å^{-1} which is a little smaller than that for the duplex DNA (Fig. 4) [11–13,25]. This might be attributed to the difference in the tunneling energy between the donor or acceptor and bridge states [26,27], or to the structure of the hairpin ODN containing the consecutive A sequence.
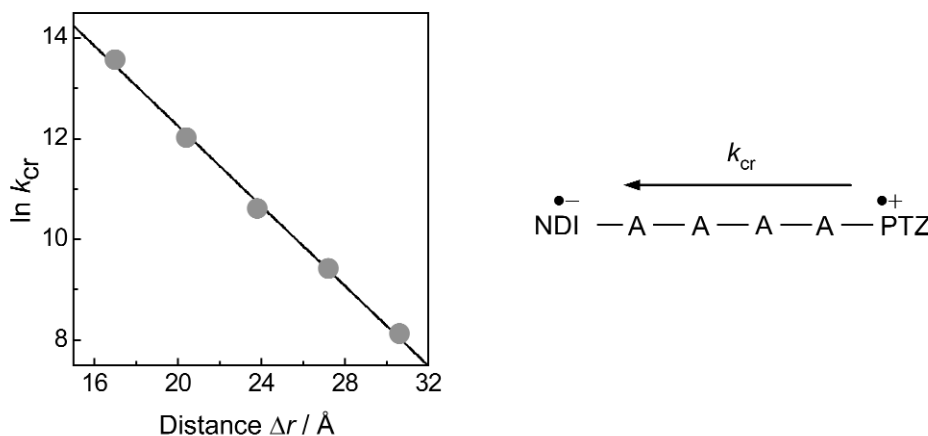

Fig. 4 A plot of $\ln k_{cr}$ against the distance between NDI and PTZ (Δr).

Assuming that the final charge-separated state is accomplished by the process in which a hole generated on the A base migrates to PTZ via the A-hopping (Fig. 2), the correlation between the rate constants (k_A, k_1, k_2) and charge separation yields (Φ_{cs}) is expressed by eq. 3 [28],

$$\Phi' = \frac{\Phi_{cs}}{1 - \Phi_{cs}} = \frac{\left(k_2/k_1\right)}{1 + \left(N-1\right)\left(k_2/k_A\right)} \qquad (3)$$

where k_A, k_1, and k_2 are the rate constants of the A-hopping, charge recombination between NDI$^{\bullet-}$ and A$^{\bullet+}$, and the hole shift from adjacent A$^{\bullet+}$ to PTZ, respectively. The electron-transfer process from ^{1}NDI* to nucleobases and charge recombination between the nucleobase radical cation and NDI$^{\bullet-}$ were previously reported by Lewis and coworkers, demonstrating that the charge separation and recombination rates between NDI and the A–T pair were 7.3×10^{12} s^{-1} and $k_1 = 2.5 \times 10^{11}$ s^{-1}, respectively [17]. The rate constants for the A-hopping process were obtained by fitting Φ_{cs} depending on the hopping number (N) to eq. 3 using the k_1 value of 2.5×10^{11} s^{-1} to provide the k_A of 10^{10} s^{-1} (Fig. 5). This value of k_A is much larger than that of hopping from G$^{\bullet+}$ to GG across one A base (5×10^7 s^{-1}) [10]. This difference is attributed to the shorter distance and the direct stacking between the A bases for the A-hopping presented in this study.

In this section, kinetic study of charge separation and charge recombination in synthetic hairpin ODN was described. Two different processes were observed for the charge transfer across the identical
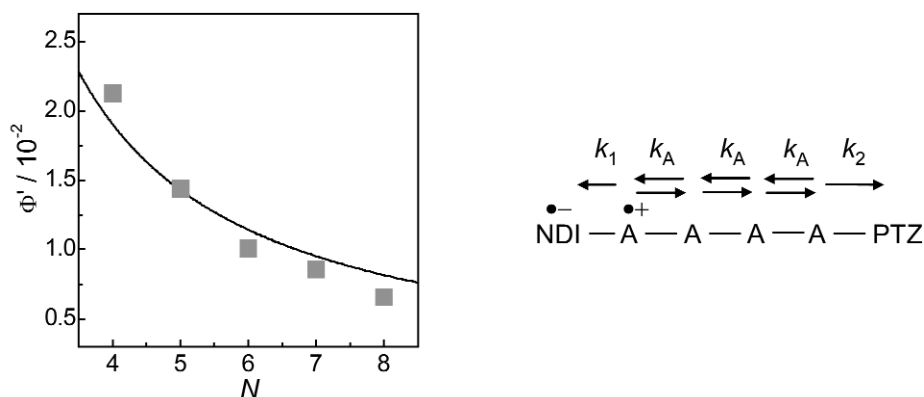
Fig. 5 Dependence of quantum yields ratio (Φ') for the charge separation upon the number of the hopping steps (N).

(A)$_n$-bridge in DNA. In the case of charge separation, since ^{1}NDI* oxidizes A, a hole is generated at A nearest to NDI and hole transfer proceeds by the A-hopping. Whereas, PTZ$^{\cdot+}$ cannot oxidize A, resulting in the charge recombination by the single-step superexchange mechanism across (A)$_n$-bridge between NDI$^{\cdot-}$ and PTZ$^{\cdot+}$. These results clearly show that the mechanism of hole transfer in DNA strongly depends on the redox nature of the oxidant, whether it produces only G$^{\cdot+}$ or both A$^{\cdot+}$ and G$^{\cdot+}$. The rate constant of the A-hopping was determined to be 10^{10} s^{-1} by analyzing the obtained charge separation yields, and A-hopping proceeds faster than 10^8 s^{-1} over the distance of 23 Å. It was demonstrated that fast and weak distance-dependent A-hopping causes a long-lived charge-separated state in DNA. The effect of A oxidation and subsequent A-hopping on the photosensitized DNA damage is discussed in the next section.

LIFETIME OF CHARGE-SEPARATED STATE AND PHOTOSENSITIZED DNA DAMAGE

The photoirradiation of DNA-bound Sens produces the radical anion of the Sens (Sens$^{\cdot-}$) and DNA radical cation (DNA$^{\cdot+}$) as the charge-separated state through photoinduced electron transfer [29]. The efficiency of the photoinduced one-electron oxidation of DNA is seemingly low since the charge recombination rate is usually much faster than the process leading to the DNA strand cleavage, such as the reaction of G$^{\cdot+}$ with water [10,13,30]. Hole transfer by G-hopping is also too slow to compete with charge recombination. However, the photosensitized DNA damage does occur [31]. In the previous section, we reported the kinetics of hole transfer in DNA by the A-hopping, which is weakly distance-dependent and proceeds faster than 10^8 s^{-1} over the distance range of 7–22 Å [18,32]. These findings prompted us to suggest that a fast hole transfer by A-hopping may help to separate the hole and Sens$^{\cdot-}$ during the photosensitized one-electron oxidation of DNA, providing the time for G$^{\cdot+}$ and Sens$^{\cdot-}$ to react with water or O$_2$. Here, to assess this hypothesis, the laser flash photolysis and high-performance liquid chromatography (HPLC) analysis of NDI-modified ODNs were performed [33].

NDI was selected as a Sens since ^{1}NDI* can oxidize A to promote hole transfer by the A-hopping to eventually yield G$^{\cdot+}$ [18,19,25,34,35]. Several ODNs with different distances between the NDI and Gs with intervening A$_n$ sequences (NDn) were synthesized, and the effect of the hole transfer on the DNA damage was investigated (Table 2). The excitation of NDI-modified ODN with the 355-nm laser (5 ns, 5 mJ pulse^{-1}) produced NDI$^{\cdot-}$ and ODN$^{\cdot+}$ charge-separated state through the photoinduced electron transfer, and the charge separation and recombination processes were examined by monitoring the formation and decay of NDI$^{\cdot-}$ as shown in Fig. 6. In the case of NDn ($n = 0$–2) where Gs are near the NDI, no transient absorption was observed due to the fast charge separation and charge recombination which proceed within the laser flash duration of 5 ns. In NDn ($n = 3$–5) where the Gs are separated from

NDI by more than three base pairs, the formation of the transient absorption with a maximum peak at 495 nm was observed immediately after the flash excitation, which was assigned to NDI$^{\bullet-}$ [19]. The yield of the formed NDI$^{\bullet-}$ was similar for NDn (n = 3–5). In contrast, the lifetime of the charge-separated state significantly increased with the increasing of the distance between NDI and Gs, i.e., the charge recombination process is strongly distance-dependent. These results are consistent with the charge separation by the A-hopping and charge recombination by the superexchange mechanism as described in the previous section [14,15,32,36–38]. The charge separation yield is small at about 2 % [18] owing to the fast charge recombination from the contact radical ion pair [39]. Therefore, the charge-separated state is generated by occasional escape from the charge recombination by the hole shift process. However, once a hole escapes from the Coulombic interaction, it efficiently migrates through DNA by the A-hopping [18]. Insertion of a single G in the A$_n$ sequence between NDI and Gs significantly diminished the transient absorption of NDI$^{\bullet-}$ (NDG), since the inserted G serves as a hole trap on the hole shift process causing inhibition of consecutive A-hopping in which a hole migrates to Gs [40,41].

Table 2 Decay lifetime of NDI$^{\bullet-}$ and consumption of G in the photosensitized DNA damage.

| ODNs	Sequence	τ (μs)[b]	–G (%)[c]
ND0	$^{5'}$NDI–CGCGCTTTTT		
	$^{3'}$GCGCGAAAAA	<0.005	<0.1
ND1	$^{5'}$NDI–TCGCGCTTTT		
	$^{3'}$AGCGCGAAAA	<0.005	<0.1
ND2	$^{5'}$NDI–TTCGCGCTTT		
	$^{3'}$AAGCGCGAAA	<0.005	<0.1
ND3	$^{5'}$NDI–TTTCGCGCTT		
	$^{3'}$AAAGCGCGAA	0.24	0.36
ND4	$^{5'}$NDI–TTTTCGCGCT		
	$^{3'}$AAAAGCGCGA	0.20 (48), 7.1 (52)	2.6
ND5	$^{5'}$NDI–TTTTTCGCGC		
	$^{3'}$AAAAAGCGCG	6.0 (31), 60 (69)	10
NDG	$^{5'}$NDI–TCTTTTGCGC		
	$^{3'}$AGAAAACGCG	<0.005	1.5

[a]Laser flash photolysis was carried out in an aqueous solution containing 40 μM ODN (strand conc.) and 20 mM pH 7.0 Na phosphate buffer.
[b]The decay lifetime of NDI$^{\bullet-}$ (preexponential).
[c]ODNs were photoirradiated with 355-nm laser (1.6 mJ pulse^{-1}, 1500 pulses, total irradiated energy of 2.4 J), digested with snake venom phosphodiesterase/nuclease P1/alkaline phosphatase to 2'-deoxyribonucleosides. The consumption of G was quantified by HPLC using A as an internal standard.

To investigate the effect of the hole transfer on the DNA damage during the photosensitized one-electron oxidation of DNA, NDn was photoirradiated and the consumption of G was quantified by HPLC (Table 2). Interestingly, the consumption of G increased with the increasing of the distance between NDI and Gs. In the case of NDG, where most of the generated holes recombine within the laser duration because of the inserted G in the A$_n$ sequence, the consumption of G was small even though the remaining Gs locate far from NDI. Thus, not the distance between the NDI and Gs, but the lifetime of the charge-separated state determines the efficiency of the DNA damage. In other words, the yield of the DNA damage increases with the increase in the lifetime of the charge-separated state.

The combination of the transient absorption measurement and DNA damage quantification provide the data for the effects of the hole transfer on the DNA damage during the photosensitized one-electron oxidation of DNA. For the Sens, which can only oxidize G, the close distance between the Sens and G is crucial for the efficient DNA damage [9,42]. In contrast, in the case of Sens, which can also
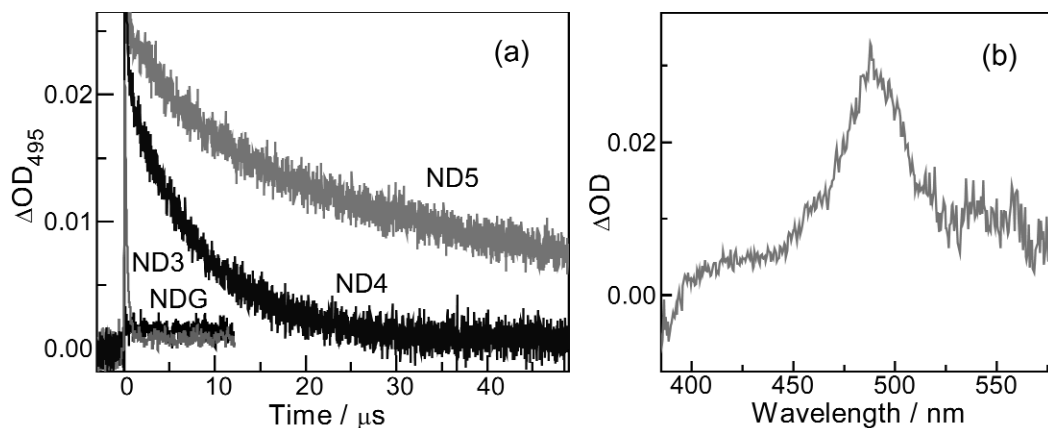
Fig. 6 (a) Time profiles of the transient absorption of NDI$^{\cdot-}$ monitored at 495 nm during the 355-nm laser flash photolysis of Ar-saturated aqueous solution of NDI-modified ODNs: NDn (n = 3–5), and NDG. (b) The transient absorption spectrum of NDI$^{\cdot-}$ obtained at 100 ns after the 355-nm flash excitation of ND3.

oxidize A to promote the hole transfer by the A-hopping, the shorter distance between the Sens and G is not necessary for the efficient DNA damage. This is also true in the case of Schuster's work where anthraquinone was used as the Sens, which can also oxidize A [43,44]. Our results strongly suggest that the hole transfer plays an important role in separating Sens$^{\cdot-}$ and G$^{\cdot+}$ during the photosensitized one-electron oxidation of DNA, providing a sufficiently long time for G$^{\cdot+}$ and Sens$^{\cdot-}$ to react with water or O$_2$, avoiding the charge recombination and making the reaction irreversible.

TWO-COLOR, TWO-LASER DNA DAMAGE

Photodynamic therapy is a promising treatment for cancer based on a photosensitized oxidative reaction at the diseased tissues producing cell death, and membrane, protein, and DNA are considered as a potential target [3,45]. Compared with surgery and chemotherapy, the combination of Sens uptake in malignant tissues and selective light delivery offers the advantage of a selective method of destroying diseased tissues without damaging surrounding healthy tissues. Following the absorption of light, Sens is activated to the singlet excited state, ^{1}Sens*, which may convert to the triplet excited state, ^{3}Sens*. The mechanisms of tumor destruction involve oxidation through electron transfer from cellular component to ^{1}Sens* or ^{3}Sens* (mechanism Type I), as well as oxidation mediated by singlet oxygen (mechanism Type II), which is formed through energy transfer from ^{3}Sens* to molecular oxygen [46]. When targeting DNA, the binding of Sens to DNA will favor the Type I process, as the close association of Sens to DNA is important in the photoinduced one-electron oxidation of DNA [31]. Excitation of DNA-bound Sens produces the Sens$^{\cdot-}$/DNA$^{\cdot+}$ (ultimately yielding G$^{\cdot+}$ by hole transfer) charge-separated state through photoinduced electron transfer. However, the efficiency of producing photosensitized DNA damage is low because of the charge recombination [10,29,37,40]. Thus, the absorption of a photon by Sens occasionally leads to DNA damage, but only with the aid of hole transfer, which provides time for DNA$^{\cdot+}$ and Sens$^{\cdot-}$ to react with water or O$_2$ [14,33,41–44,47]. Here, we report the first study of nanosecond-laser DNA damage, using a combination of two-color pulses as a promising new strategy to reach a high DNA-damaging efficiency. The first laser pulse was applied for the production of the Sens$^{\cdot-}$ and DNA$^{\cdot+}$, and the second laser pulse for the electron ejection from Sens$^{\cdot-}$ [48], making the reaction irreversible [49].

The proposed two-color, two-laser DNA damage is represented as a two-step process in a simplified scheme (Fig. 7). In this study, NDI was used as a Sens that can be excited with a first laser at a wavelength of 355 nm [17,19,34,50,51]. First, to assess the feasibility of electron ejection from Sens$^{\cdot-}$
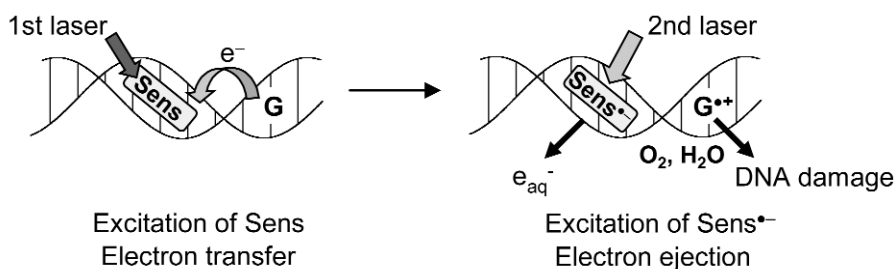
Fig. 7 Schematic representation of two-color, two-laser DNA damage.

bound to DNA, a pulse radiolysis-laser flash photolysis of NDI-conjugated ODN (NDI–ODN) was performed (Fig. 8) [32,52]. NDI$^{\bullet-}$ with a maximum absorption peak at 495 nm [19] was generated from electron attachment during the pulse radiolysis of NDI–ODN. Since Sens$^{\bullet-}$ often absorbs light at a longer wavelength compared with its nonreduced form, laser pulses with a longer wavelength can be used for the excitation of Sens$^{\bullet-}$, and a 532-nm laser was applied as the second laser. Irradiation of NDI$^{\bullet-}$ in NDI–ODN with a 532-nm laser pulse caused a decrease in ΔOD of NDI$^{\bullet-}$, and the formation of absorption at 630 nm assigned to a solvated electron (e_{aq}^-) immediately after the flash (inset), demonstrating the successful electron ejection from NDI$^{\bullet-}$ to the solvent water.
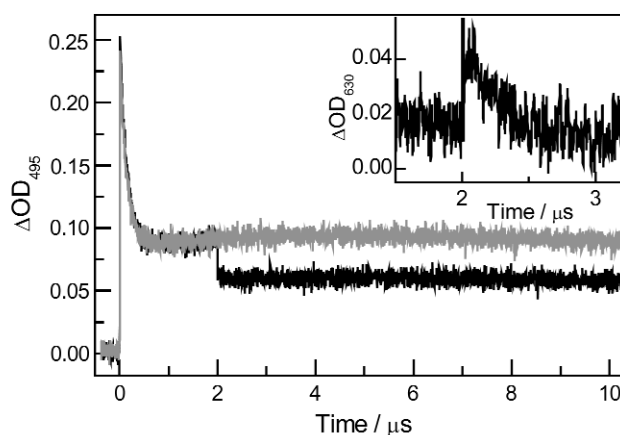
Fig. 8 Electron ejection from NDI$^{\bullet-}$ promoted by a 532-nm laser pulse. NDI$^{\bullet-}$ was generated from electron attachment during the pulse radiolysis of NDI–ODN (NDI–AAAAAAGTGCGC/TTTTTTCACGCG) (gray), and photoirradiated with a 532-nm laser pulse at 2 μs after the electron pulse (black). Inset: Formation and decay of the solvated electron monitored at 630 nm.

To test the efficiency of two-color, two-laser irradiation for DNA damage, the consumption of G upon two-color, two-laser irradiation of ODN–G and ODN–GG bound to added *N,N′*-bis-[3-(*N*-dimethyl)propyl]-1,4,5,8-naphthaldiimide dichloridite (NDI–HCl), and NDI–ODN was compared with that of single-laser experiments. It is of special interest that an increase in the consumption of G was observed with the combination of the first and second laser irradiations compared with irradiation by the 355-nm pulses alone (Table 3). Using 532-nm pulses alone, there is no DNA damage, as this would require a nonresonant two-photon excitation, since neither nonreduced NDI nor DNA absorbs above 450 nm [53,54]. Hence, the second laser alone cannot damage DNA, but does provide enough additional energy to cross the ionization threshold of NDI$^{\bullet-}$, removing the electron to the solvent and making the reaction irreversible [48]. Compared with ODN–G, a higher consumption of G was observed for ODN–GG where the ionization potential of G is lowered by a stacking interaction between Gs [55],

demonstrating that the consumption of G is based on the photoinduced electron transfer by the first laser. The acceleration of DNA damage by the second laser was the highest for ODN covalently bonded with NDI where the sequence was designed to generate a hole selectively on A and to have a lifetime of charge-separated state in the order of 100 ns [18,33]. Figure 9 shows the time profile of NDI$^{\bullet-}$ in the one-color laser photolysis of NDI–ODN. Upon the first laser excitation, hole transfer via consecutive fast A-hopping leads to a charge-separated state within the laser duration (5 ns), and the charge recombination proceeds by the single-step superexchange from G$^{\bullet+}$ about 14 Å away from NDI$^{\bullet-}$ with a lifetime of 240 ns [18,29,33]. Also shown in Fig. 9 is the consumption of G as a function of the delay time of the second laser pulse in the time-delayed two-color photolysis. The delay time dependence of the consumption of G agreed well with the decay of the transient absorption of NDI$^{\bullet-}$ obtained in the one-color laser photolysis. Thus, the acceleration caused by the second laser is clearly based on the excitation of NDI$^{\bullet-}$. The experiments were performed under low-conversion conditions, and the consumption of G was linearly correlated with the irradiation time and the power of the second laser in the present experimental arrangement.

Table 3 Consumption of G in the photosensitized damage of ODNs.[a]

| ODN		–G (%)[a]		
		355 nm	532 nm	355 + 532 nm
ODN–G[b]	(TG)$_6$T /(AC)$_6$A	0.6	<0.3	2.6
ODN–GG[b]	(TTGG)$_3$T /(AACC)$_3$A	2.5	<0.2	16.7
NDI–ODN[c]	NDI-T$_3$CGCGCT$_2$ /A$_3$GCGCGA$_2$	0.8	0	14.2

Laser flash photolysis was carried out in an aqueous solution containing 40 μM ODN (strand conc.) and 20 mM pH 7.0 Na phosphate buffer. In the case of ODN–G and ODN–GG, 40 μM of NDI–HCl was added. For the two-wavelength irradiation, the 532-nm laser pulse (20 mJ/pulse) was synchronized with the 355-nm laser pulse (1.6 mJ/pulse) with a 10-ns delay.
[a]Photoirradiated ODNs were digested with snake venom phosphodiesterase/nuclease P1/alkaline phosphatase to 2'-deoxyribonucleosides and the consumption of G was quantified by HPLC using A as an internal standard.
[b]Photoirradiated for 20 min (355 nm 19 J, 532 nm 240 J).
[c]Photoirradiated for 5 min (355 nm 4.8 J, 532 nm 60 J).

In the present study, it was demonstrated that a combination of nanosecond laser pulses at two different colors increases DNA damage. This strategy has the advantage that the intensity of the 355-nm pulses in the first step can be kept low, and a high DNA damaging efficiency can be attained by applying the second laser pulse at a longer wavelength with a greater depth of tissue penetration due to reduced scattering and minimal absorption from nonpharmacological chromophores in the tissue. Two-color irradiation also offers spatial control of the reaction at the focal point of the lasers [56–60]. The photosensitizer NDI used in this preliminary experiment is not adequate for practical use since the charge-separation yield is small at about 2 % owing to the fast charge recombination from the contact radical ion pair [18,39]. Therefore, a second laser exerts its effect only on NDI$^{\bullet-}$ generated by occasional escape from the charge recombination by hole transfer. Thus, in order for efficient oxidative DNA cleavage to occur, it is necessary to increase the charge-separation yield by decreasing the rate constant for charge recombination. This can be achieved by the use of triplet sensitizers [31], and by hole generation on A to promote fast hole transfer by an A-hopping mechanism that helps to separate the hole and Sens$^{\bullet-}$ [32,33].
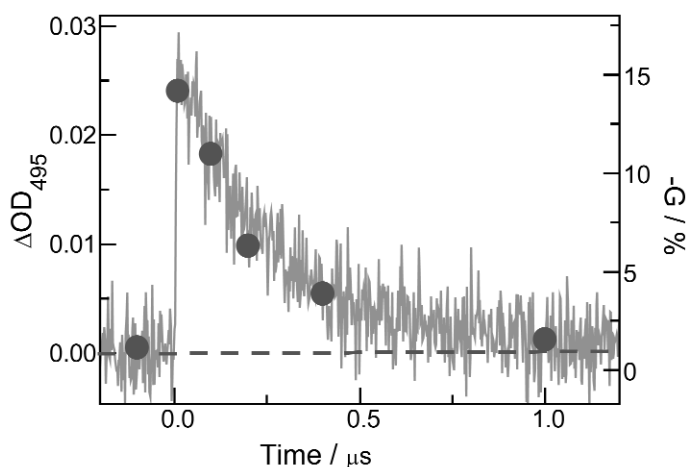
Fig. 9 Formation and decay of NDI$^{\cdot-}$ and the effect of the delay time between two laser pulses on the consumption of G during the laser flash photolysis of NDI–ODN (NDI–TTTCGCGCTT/AAAGCGCGAA). The transient absorption of NDI$^{\cdot-}$ was monitored at 495 nm following 355-nm excitation (left axis). The consumption of G is plotted as a function of the delay of the 532-nm pulse with respect to the 355-nm pulse (●: right axis). The dashed line shows the consumption of G in the absence of the 532-nm pulse.

CONCLUSIONS

In the present article, the kinetics of hole transfer in DNA by the A-hopping and its effect on the photosensitized DNA damage was investigated by the transient absorption measurement, and DNA damage quantification using HPLC. It was demonstrated that the hole generated on A rapidly migrates through DNA by hopping between As with a rate constant faster than 10^8 s^{-1} over the distance range of ~22 Å. The rate constant of the each A-hopping process between adjacent As was determined to be ~10^{10} s^{-1} from an analysis of the yield of the charge separation depending on the number of A-hopping steps. This fast and weak distance-dependent hole transfer by A-hopping was shown to generate a long-lived charge-separated state in DNA. When photoinduced electron transfer occurs between excited Sens and A, a part of a hole escapes from the initial charge recombination via consecutive A-hopping to be trapped at G. Once G$^{\cdot+}$ is formed far from Sens$^{\cdot-}$, charge recombination proceeds by either super-exchange or A-hopping following slow A oxidation by G$^{\cdot+}$, producing a long-lived charge-separated state. These results suggested that a hole transfer by the A-hopping may help to separate the hole and Sens$^{\cdot-}$ during the photosensitized one-electron oxidation of DNA, providing a sufficiently long time for G$^{\cdot+}$ and Sens$^{\cdot-}$ to react with water or O$_2$. The yield of the DNA damage correlates well with the lifetime of the charge-separated state during the photosensitized one-electron oxidation of DNA, demonstrating that A oxidation in the consecutive A sequences is crucial for the photosensitized DNA damage. Our results suggest that consecutive A sequences may serve as a good target in photosensitized DNA damage in photodynamic therapy, or G adjacent to such sequences may be potential hot spots of oxidative DNA damage. These kinetic studies of photosensitized DNA damage allowed us to propose a new method for efficient photosensitized DNA damage, which is based on the two-color, two-laser irradiation. The first laser pulse was applied for the production of the Sens$^{\cdot-}$ and DNA$^{\cdot+}$, and the second laser pulse for the electron ejection from Sens$^{\cdot-}$, making the reaction irreversible and increasing the DNA damage yield.

ACKNOWLEDGMENTS

REFERENCES

1. K. Kino and H. Sugiyama. *Chem. Biol.* **8**, 369–378 (2001).
2. S. Shibutani, M. Takeshita, A. P. Grollman. *Nature* **349**, 431–434 (1991).
3. D. E. J. G. J. Dolmans, D. Fukumura, R. K. Jain. *Nat. Rev. Cancer* **3**, 380–387 (2003).
4. C. A. M. Seidel, A. Schulz, M. H. M. Sauer. *J. Phys. Chem.* **100**, 5541–5553 (1996).
5. S. Steenken and S. V. Jovanovic. *J. Am. Chem. Soc.* **119**, 617–618 (1997).
6. E. Meggers, M. E. Michel-Beyerle, B. Giese. *J. Am. Chem. Soc.* **120**, 12950–12955 (1998).
7. P. T. Henderson, D. Jones, G. Hampikian, Y. Z. Kan, G. B. Schuster. *Proc. Natl. Acad. Sci. USA* **96**, 8353–8358 (1999).
8. M. E. Nunez, D. B. Hall, J. K. Barton. *Chem. Biol.* **6**, 85–97 (1999).
9. K. Nakatani, C. Dohno, I. Saito. *J. Am. Chem. Soc.* **121**, 10854–10855 (1999).
10. F. D. Lewis, X. Y. Liu, J. Q. Liu, S. E. Miller, R. T. Hayes, M. R. Wasielewski. *Nature* **406**, 51–53 (2000).
11. F. D. Lewis, T. F. Wu, Y. F. Zhang, R. L. Letsinger, S. R. Greenfield, M. R. Wasielewski. *Science* **277**, 673–676 (1997).
12. C. Z. Wan, T. Fiebig, O. Schiemann, J. K. Barton, A. H. Zewail. *Proc. Natl. Acad. Sci. USA* **97**, 14052–14055 (2000).
13. K. Kawai, T. Takada, S. Tojo, N. Ichinose, T. Majima. *J. Am. Chem. Soc.* **123**, 12688–12689 (2001).
14. B. Giese, J. Amaudrut, A. K. Kohler, M. Spormann, S. Wessely. *Nature* **412**, 318–320 (2001).
15. T. Kendrick and B. Giese. *Chem. Commun.* 2016–2017 (2002).
16. N. Rahe, C. Rinn, T. Carell. *Chem. Commun.* 2120–2121 (2003).
17. F. D. Lewis, R. S. Kalgutkar, Y. S. Wu, X. Y. Liu, J. Q. Liu, R. T. Hayes, S. E. Miller, M. R. Wasielewski. *J. Am. Chem. Soc.* **122**, 12346–12351 (2000).
18. T. Takada, K. Kawai, X. Cai, A. Sugimoto, M. Fujitsuka, T. Majima. *J. Am. Chem. Soc.* **126**, 1125–1129 (2004).
19. J. E. Rogers, S. J. Weiss, L. A. Kelly. *J. Am. Chem. Soc.* **122**, 427–436 (2000).
20. K. Kawai, T. Takada, S. Tojo, T. Majima. *Tetrahedron Lett.* **43**, 89–91 (2002).
21. F. D. Lewis, X. Zuo, J. Liu, R. T. Hayes, M. R. Wasielewski. *J. Am. Chem. Soc.* **124**, 4568–4569 (2002).
22. T. Takada, K. Kawai, S. Tojo, T. Majima. *J. Phys. Chem. B* **107**, 14052–14057 (2003).
23. T. T. Williams, D. T. Odom, J. K. Barton. *J. Am. Chem. Soc.* **122**, 9048–9049 (2000).
24. F. D. Lewis, J. Liu, X. Liu, X. Zuo, R. T. Hayes, M. R. Wasielewski. *Angew. Chem., Int. Ed.* **41**, 1026–1028 (2002).
25. F. D. Lewis, R. L. Letsinger, M. R. Wasielewski. *Acc. Chem. Res.* **34**, 159–170 (2001).
26. F. D. Lewis, J. Liu, W. Weigel, W. Rettig, I. V. Kurnikov, D. N. Beratan. *Proc. Natl. Acad. Sci. USA* **99**, 12536–12541 (2002).
27. F. D. Lewis, Y. Wu, R. T. Hayes, M. R. Wasielewski. *Angew. Chem., Int. Ed.* **41**, 3485–3487 (2002).
28. M. Bixon, B. Giese, S. Wessely, T. Langenbacher, M. E. Michel-Beyerle, J. Jortner. *Proc. Natl. Acad. Sci. USA* **96**, 11713–11716 (1999).

29. F. D. Lewis, J. Liu, X. Zuo, R. T. Hayes, M. R. Wasielewski. *J. Am. Chem. Soc.* **125**, 4850–4861 (2003).
30. V. Shafirovich, J. Cadet, D. Gasparutto, A. Dourandin, W. D. Huang, N. E. Geacintov. *J. Phys. Chem. B* **105**, 586–592 (2001).
31. B. Armitage. *Chem. Rev.* **98**, 1171–1200 (1998).
32. K. Kawai, T. Takada, S. Tojo, T. Majima. *J. Am. Chem. Soc.* **125**, 6842–6843 (2003).
33. K. Kawai, T. Takada, T. Nagai, X. Cai, A. Sugimoto, M. Fujitsuka, T. Majima. *J. Am. Chem. Soc.* **125**, 16198–16199 (2003).
34. J. E. Rogers and L. A. Kelly. *J. Am. Chem. Soc.* **121**, 3854–3861 (1999).
35. D. A. Vicic, D. T. Odom, M. E. Nunez, D. A. Gianolio, L. W. McLaughlin, J. K. Barton. *J. Am. Chem. Soc.* **122**, 8603–8611 (2000).
36. B. Giese and A. Biland. *Chem. Commun.* 667–672 (2002).
37. B. Giese and M. Spichty. *ChemPhysChem* **1**, 195–198 (2000).
38. C. Dohno, A. Ogawa, K. Nakatani, I. Saito. *J. Am. Chem. Soc.* **125**, 10154–10155 (2003).
39. F. D. Lewis, X. Liu, S. E. Miller, R. T. Hayes, M. R. Wasielewski. *J. Am. Chem. Soc.* **124**, 14020–14026 (2002).
40. C. Dohno, E. D. A. Stemp, J. K. Barton. *J. Am. Chem. Soc.* **125**, 9586–9587 (2003).
41. J. Yoo, S. Delaney, E. D. A. Stemp, J. K. Barton. *J. Am. Chem. Soc.* **125**, 6640–6641 (2003).
42. B. Giese. *Acc. Chem. Res.* **33**, 631–636 (2000).
43. L. Sanii and G. B. Schuster. *J. Am. Chem. Soc.* **122**, 11545–11546 (2000).
44. G. B. Schuster. *Acc. Chem. Res.* **33**, 253–260 (2000).
45. E. F. G. Dickson, R. L. Goyan, R. H. Pottier. *Cell. Mol. Biol.* **48**, 939–954 (2002).
46. W. M. Sharman, C. M. Allen, J. E. van Lier. *Methods Enzymol.* **319**, 376–400 (2000).
47. T. T. Williams, C. Dohno, E. D. A. Stemp, J. K. Barton. *J. Am. Chem. Soc.* **126**, 8148–8158 (2004).
48. M. Goez, V. Zubarev, G. Eckert. *J. Am. Chem. Soc.* **120**, 5347–5348 (1998).
49. K. Kawai, X. Cai, A. Sugimoto, S. Tojo, M. Fujitsuka, T. Majima. *Angew. Chem., Int. Ed.* **43**, 2406–2409 (2004).
50. K. Kawai, Y. Wata, M. Hara, S. Tojo, T. Majima. *J. Am. Chem. Soc.* **124**, 3586–3590 (2002).
51. K. Kawai, Y. Wata, N. Ichinose, T. Majima. *Angew. Chem., Int. Ed.* **39**, 4327–4329 (2000).
52. A. Ishida, M. Fukui, H. Ogawa, S. Tojo, T. Majima, S. Takamuku. *J. Phys. Chem.* **99**, 10808–10814 (1995).
53. C. E. Crespo-Hernandez, R. Arce. *J. Phys. Chem. B* **107**, 1062–1070 (2003).
54. T. Douki, D. Angelov, J. Cadet. *J. Am. Chem. Soc.* **123**, 11360–11366 (2001).
55. H. Sugiyama and I. Saito. *J. Am. Chem. Soc.* **118**, 7063–7068 (1996).
56. A. Ouchi, Z. Li, M. Sakuragi, T. Majima. *J. Am. Chem. Soc.* **125**, 1104–1108 (2003).
57. X. Cai, M. Hara, K. Kawai, S. Tojo, T. Majima. *Chem. Commun.* 222–223 (2003).
58. C. Russmann, J. Stollhof, C. Weiss, R. Beigang, M. Beato. *Nucleic Acids Res.* **26**, 3967–3970 (1998).
59. V. Y. Shafirovich, A. Dourandin, N. P. Luneva, N. E. Geacintov. *J. Phys. Chem. B* **101**, 5863–5868 (1997).
60. O. I. Kovalsky, I. G. Panyutin, E. I. Budowsky. *Photochem. Photobiol.* **52**, 509–17 (1990).